Planetary and Space Science 208 (2021) 105355

Contents lists available at ScienceDirect

Planetary and Space Science

journal homepage: www.elsevier.com/locate/pss

Identifying optimal working conditions for close-up imagining during the ExoMars rover mission

Tomaso R.R. Bontognali [a,b,*], Yardena Meister [b], Brigitte Kuhn [b], Jean-Luc Josset [a], Beda A. Hofmann [c,d], Nikolaus Kuhn [b,**]

[a] Space Exploration Institute, 68 Faubourg de l'Hôpital, 2000, Neuchâtel, Switzerland
[b] University of Basel, Department of Environmental Sciences, Physical Geography and Environmental Change, Klingelbergstrasse 27, 4056, Basel, Switzerland
[c] Natural History Museum Bern, Bernastrasse 15, 3005, Bern, Switzerland
[d] University of Bern, Geological Institute, Baltzerstrasse 1+3, 3012, Bern, Switzerland

ARTICLE INFO

Keywords:
Mars yard
ExoMars
Close-up imaging
Planetary exploration
Analogue testing
Science operations

ABSTRACT

A Close-Up Imager named CLUPI is one of the instruments that will be onboard the Rosalind Franklin rover, a robot that will explore the surface of Mars in the framework of the ESA/Roscosmos ExoMars mission. CLUPI will be principally used for acquiring close-up images of rock textures and sedimentary structures, identifying materials that may record information about the hypothetical existence of past microbial life. Although the technical specifications of CLUPI are well known, it is not possible to readily translate such specifications in terms of feasibility to recognize "textures of interest" at a given distance under specific light conditions on Mars. Accurate predictions are important for making fast and informed decisions during the daily tactical planning of the rover. Here, we describe the results of some mission-preparation activities, during which a commercial camera that allows for producing images analogue to those of CLUPI has been used to photograph rock samples in an indoor facility (i.e., the Marslabor of the University of Basel) that has been built *ad hoc* for simulating a Martian landscape. By varying the working distance and light conditions it has been possible to perform a preliminary assessment of the minimal-working-distance required for interpreting rock textures and sedimentary structures that are potentially present on Mars, including textures that allow for differentiating sedimentary rocks from igneous rocks, grains that allow for classifying sedimentary rocks based on their granulometry, and stromatolitic laminations representing morphological biosignatures. In general, the results suggest that rock textures tend to be recognizable even from distances that exceed those one would predict based on the resolution of the instrument and the size of the structure or particles that defines the rock texture or sedimentary structure. We also show that the angle between the illumination axis (i.e., the direction of incident light) and the target surface plays a significant role for the recognition of textural and compositional heterogeneities within the acquired images. The produced data represents a first step in identifying ideal CLUPI working-distances and illumination, and in preparing an image database that will be of help for optimizing rover operations and the scientific return of CLUPI during the ExoMars mission.

1. Introduction

ExoMars is an astrobiology joint space program from the European Space Agency (ESA) and the Russian Space Agency Roscosmos searching for evidence of life on Mars (Vago et al., 2017). The program comprises two missions: the first, launched in 2016, includes an orbiter that is currently deployed (Vago et al., 2015), the second, with a launch date of 2022, will feature a rover (Fig. 1A) and a platform equipped with a suite of scientific instruments for investigating the surface and the subsurface of Mars. One of the scientific instruments on board the rover – CLUPI (for Close-UP Imager) – is a camera system designed to acquire high-resolution, color images of rocks, soils, drill fines and drill core samples (Fig. 1B & C) (Josset et al., 2017). The visual information produced by CLUPI is comparable to that a geologist would obtain using a hand-lens. These images will help scientists to determine the geological context and paleoenvironment where the studied rocks were originally

* Corresponding author. Space Exploration Institute, 68 Faubourg de l'Hôpital, 2000, Neuchâtel, Switzerland.
** Corresponding author.
E-mail addresses: tomaso.bontognali@space-x.ch (T.R.R. Bontognali), nikolaus.kuhn@unibas.ch (N. Kuhn).

https://doi.org/10.1016/j.pss.2021.105355
Received 29 March 2021; Received in revised form 17 July 2021; Accepted 28 September 2021
Available online 29 September 2021

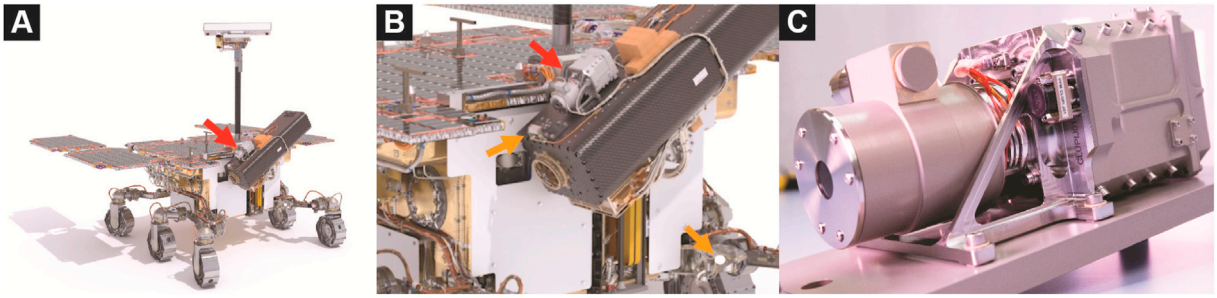

Fig. 1. The Close-Up Imager (CLUPI) on board the Rosalind Franklin ExoMars rover. (A) Computer aided drafting of the ExoMars Rover. The red arrow indicates the position where CLUPI is installed on the movable drill-box. **(B)** Close-up of Figure (A). The red arrow indicates CLUPI. The blue arrows indicate the position of the two mirrors that allow for obtaining additional fields of view, mitigating the fact that CLUPI is not installed on a dedicated movable robotic arm. (**C**) The CLUPI instrument. Image credits ESA.

formed (e.g., aqueous vs volcanic, high energy vs calm shallow waters, …) and possibly even to identify putative morphological biosignatures (Bontognali et al., 2016; Cady et al., 2003; Davies et al., 2016; Hofmann et al., 2008; Homann, 2019; Noffke, 2009; Westall et al., 2015).

At a distance of 10 cm from the object, the resolution of the CLUPI images is about 7 μm/pixel and it is possible to focus from 10 cm to infinity (Josset et al., 2017). CLUPI is fixed on the drill box of the rover (Fig. 1B). Thanks to the movements of both the rover and the drill box, CLUPI will be angled and raised so that it will be possible to acquire images from different points of view. Additional field of views will be guaranteed by two mirrors that are strategically placed one on the body of the rover and the second on the drill box (Fig. 1B) (Josset et al., 2017).

During the ExoMars mission, the science team located at the Rover Operations Control Center (ROCC) will receive a limited amount of data (on average approximately 1 full resolution CLUPI image/day), and it will have only a couple of hours for interpreting the visual information and decide how to program the activities of the rover for the subsequent 48 h. This situation, which is far more complicated than driving a rover remotely but in real-time, makes it essential to be able to interpret the transmitted data as quickly and as precisely as possible, in order to efficiently plan the rover's activity for the subsequent days. The need of obtaining images providing straightforward answers to precise scientific questions combined with the limited mobility of CLUPI (not mounted on and independent robotic arm but on the movable drill box) makes it important to conduct comprehensive preparatory activities on Earth, prior to the primary mission on Mars.

Here, we describe the steps that have been undertaken to build a testing facility we named Marslabor (Fig. 2). The facility consists of a Martian landscape equipped with a set of lights that allows for reproducing an illumination analogue to that of the surface of Mars. Then, we present a first set of simulations during which rock samples analogue to Martian rocks that are considered relevant targets for the ExoMars mission have been photographed from various distances under various light conditions, producing view areas analogue to those that will produced by the ExoMars rover. We conducted the simulations using a commercial off-the-shelf camera and lens that allowed us to obtain images with the same viewed area and pixel resolution as those of CLUPI, not with a flight-like model that has identical detector and proximity electronics, optics and focus mechanism, and color calibration process. Although the spatial resolution and the technical specifications of CLUPI are well known, without performing tests on actual geological samples it is difficult to predict what are the light conditions and the minimum distance necessary to recognize "textures of interest" with an adequate confidence. The ability of recognizing textures and sedimentary structures does not depend exclusively on the size of the defining features (e.g., particle size, thickness of the lamination) but also on attributes like the color (e.g., contrast between single grains or laminae), which in turn depend on the specific rock facies and its weathering status.

2. Methods

2.1. Marslabor of the University of Basel

The Marslabor has been established in the Technology Center Witterswil near Basel within an industrial building made available by the University of Basel (Fig. 2). Other existing "Mars yards" (e.g., Mars yard at Jet Propulsion Laboratory in Pasadena, Mars yard at the Stevenage site of Airbus Defence and Space) are mostly used to test the rover's locomotion system. The Marslabor was instead designed for acquiring images under controlled light conditions from distances up to 8 m, which is not

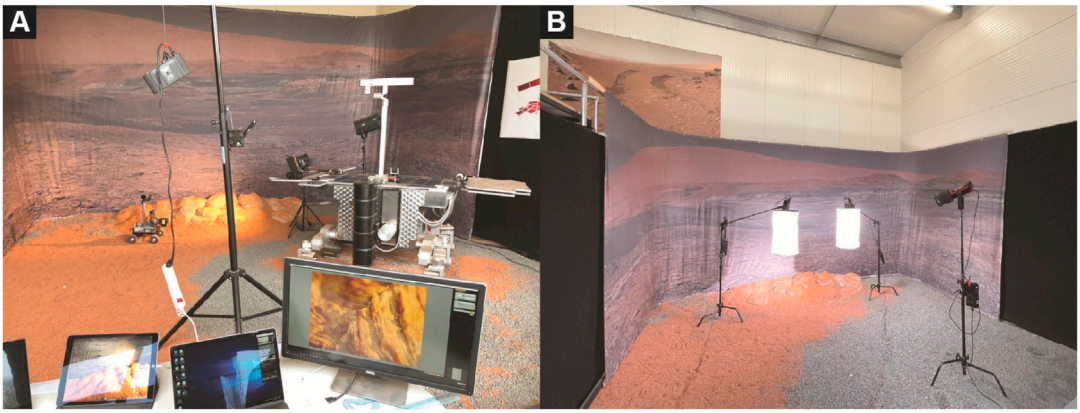

Fig. 2. Marslabor of the University of Basel located in Witterswil, Switzerland. (A) Overview of the Marslabor. A static ExoMars rover model and a small rover used for simulating remotely controlled CLUPI operations are visible in the image. **(B)** Light setup that has been used to create the direct and diffused light illumination under which the images presented in this study were acquired.

possible in most standard-size laboratories. The Marslabor consists of an 80 m^2 room with a high ceiling and includes a 40 m^2 test bed surrounded by a canvas with a printed Martian landscape. The test bed is covered with a grey basalt (i.e., leucite-tephrite from the Eifel region that has been artificially broken in fragments with a diameter of 8–10 mm) and a reddish sandstone rich in hematite (i.e., mixture of shredded bricks with a granulometry smaller than 6 mm). An artificial outcrop made of painted expanded polystyrene covered with a rendering mortar has been built and serves as a stand for displaying and photographing the samples.

The lighting of the Marslabor aims at reproducing different solar angles above the horizon and different azimuths relative to the target rock. The lighting system is comprised of the following equipment: for direct light we use a 300 W LED Daylight point source Aputure LS C300D MKII (color temperature 5500 K, 45000 LUX at 1 m) equipped with a Fresnel 2X that can produce up to 90000 LUX; for diffused light we use two 180 W LED Daylight point source (color temperature 5500 K, 7000 LUX at 1 m) combined with Space Light Aputure attachments that create a wide-spread light source. The lights are fixed on Manfrotto Avenger C-Stand tripods that can be flexibly moved around the Marslabor. Direct light and diffused light has been measured directly on the target geological samples using a light meter Sekonic Speedmaster L-858D. All the images presented in this study were acquired by adjusting the lamps position or by dimming their power in order to obtain a measured value on the sample of 5000 LUX of direct light and 1000 LUX of indirect light. The proportion among direct and indirect light has been selected according to current knowledge on Mars illumination (e.g., Appelbaum and Flood, 1990) and the limitation of the laboratory equipment. The total LUX are lower than average daylight illumination at Oxia planum – the selected landing site of the ExoMars rover. However, by increasing the intensity of the direct light, it would have not been possible to obtain a realistic proportion of 5 to 1 between direct and diffused light, which we consider more important for the purpose of our simulations than total light intensity. Indeed, if direct light is too intense with respect to diffused light, textural features due to the topography of the sample may result unnaturally overemphasized, biasing the determination of the ideal working distance necessary to recognize an interesting rock texture or sedimentary structure. High values of diffused light are more difficult to obtain in a studio with artificial light with respect to direct light.

2.2. Reference system for target surfaces, illumination axis, and optical axis

In this study, the term "target surface" refers to the plane that best describes the spatial orientation of the region of interest. For example, the target surface may be the vertical wall of an outcrop displaying stromatolitic laminations, or a ground surface covered with sand. We report the orientation of the target surface using the dip and strike notation, which is commonly used in the field of geology. The dip corresponds to the angle between a horizontal plane and the line of maximum slope in the target surface. A horizontal plane has a dip of 0°, whereas a vertical plane has a dip of 90°. If the target surface is overhanging, its dip is reported with an angle surpassing 90°. The strike is reported with angles ranging from 0° to 360°, measured from the North in clockwise direction. If the target surface is horizontal (e.g., the ground) the strike is arbitrary, and we use the value 0°. The optical axis (i.e., the "line between the camera and the center of the target surface" or the "direction from where the image is taken") is reported using a spherical coordinate system (Fig. 3), whereby the origin is the center of the target surface and the reference plane is the horizontal plane (parallel to the floor of the Marslabor), which is orthogonal to the zenith. The polar angle is measured from the zenith, and the azimuthal angle is measured from the North in clockwise direction. The illumination axis (i.e., the line between the direct light source and the center of the target surface) is reported using the same spherical coordinates system (Fig. 3) used for defining the optical axis. With the used reference system, an image is acquired orthogonally to the target surface when the dip of the target surface is equal to the inclination of the optical axis and its strike is equal to the azimuthal angle of the optical axis. Similarly, when direct light is orthogonal to the target surface, dip and strike values correspond to the polar and azimuthal angle values of the illumination axis.

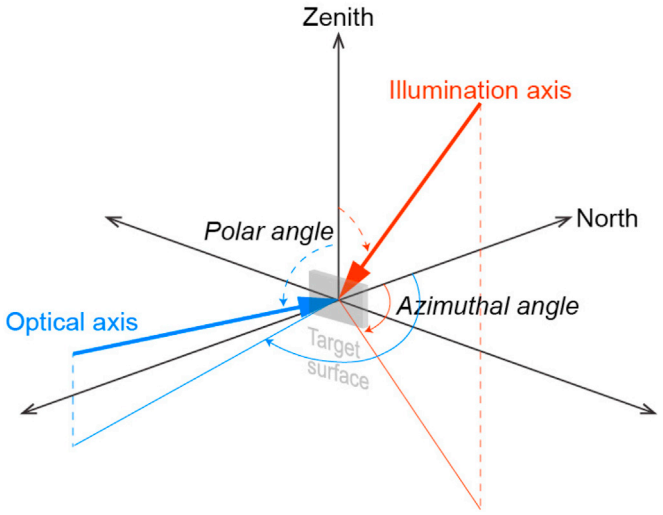

Fig. 3. Spherical reference system used to describe the optical axis (i.e., the "line between the camera and the center of the target surface") and the illumination axis (i.e., the line between the direct light source and the center of the target surface). The origin of the reference system is the center of the target surface and the reference plane is the horizontal plane (parallel to the floor of the Marslabor). The polar angle is measured from the zenith, and the azimuthal angle is measured from the North in clockwise direction. The orientation of the target surface is described using the dip and strike notation (not shown in this figure).

In this study, we have only photographed target surfaces placed vertically. Thus, the strike is always 90°. We have also artificially set the North to correspond to the back wall of the Marslabor and placed all the photographed samples parallel to it. Thus, all the target surfaces of the figures have the same dip of 90° and a strike of 180°.

2.3. Camera and image post-processing

The images on which this study is based have been taken using a Canon EOS M50 with a Canon 110 mm fixed macro lens and a mount adapter EF-EOS M. Among commercially available cameras, this body and lens combination represent one of the best analogue to the field of view (i.e., 14° ± 2° diagonal) and resolution (i.e., 2652 × 1768 x 3 pixels in color, pixel size 7.8 × 7.8 μm) of CLUPI (Josset et al., 2017). The technology and number of pixels of the Canon EOS M50 detector differs from that of the actual CLUPI instrument. To produce color images, instead of a conventional detector combined with a Bayer filter, the detector of CLUPI has three layers of pixels – red, green and blue, which results in a better "true color" spatial resolution. This is not the case with the Canon detector, in which color information is obtained using a Bayer filter and merging the information of 4 adjacent pixels. Nevertheless, CLUPI's detector has a lower resolution of 2652 × 1768 pixels with respect to M50 detector's 5196 × 3464 pixels. Thus, we assume that the lower color spatial resolution of the Canon detector is compensated by its higher pixel density, which we have subsequently subsampled obtaining the CLUPI's pixel resolution using Adobe Photoshop. Other factors (e.g., optical properties of the lenses, color calibration, etc.) are anyway at play and only a direct comparison between the EOS M50 images and those produced by CLUPI will allow for a precise assessment of the differences in image quality among the two cameras.

On the Rosalind Franklin rover, CLUPI will be accommodated on the drill box (Fig. 1A). Depending on both the position of the rover and that of the drill box, which can be rotated and raised on the vertical axis,

CLUPI will point in different directions. Two mirrors (Fig. 1B), one fixed on the rover's bracket that hold the drill box when in stowed position, and one fixed near the front end of the drill box, provide three fields of view (FOV). This solution was adopted to mitigate the fact that CLUPI is not mounted on a movable arm, like it is for example the case for the Mars Hand Lens Imager (MAHLI) on the NASA rover Curiosity (Edgett et al., 2012). The mirror placed on the drill box splits the total CLUPI field of view (FOV) in two parts, which are referred to as FOV2 and FOV3 (Josset et al., 2017). All the simulations presented in this study corresponds to CLUPI images acquired in the configuration that will be used for observing geological outcrops. In this configuration, CLUPI images correspond to FOV2, which has a resolution of 1228 X 2652 pixel. To obtain FOV2, we have cropped the EOS M50 images using Adobe Photoshop, setting 1228 X 2652 pixel as image size. The close-up presented in the figures were obtained using the "clipping mask" function of Adobe Illustrator and enlarging the region of interest without modifying the original number of pixels. Thus, the presented close-up images have the same pixel resolution that one would obtain by zooming-in into an original CLUPI image.

2.4. Rock samples selected for the simulations

The choice of the rock samples used for these simulations was not directly based on the existing information about the geology of the landing site (i.e., Oxia Planum) and the likelihood that such facies will be detected by the rover during the ExoMars mission (e.g., Quantin-Nataf et al., 2021; Mandon et al., 2021). Rather, our goal was to include representative examples of a variety of textures (e.g., coarse-grained vs fine-grained) and sedimentary structures (e.g., laminated vs non-laminated) in a selection of only few samples. Considering that the main goal of the ExoMars mission is that of searching for evidence for the existence of past life, rover operations will focus on identifying rocks that have a high potential of preserving any type of biosignatures (Vago et al., 2017). Although exceptions exist and some biosignatures may be associated to igneous rocks (Ross and Fisher, 1986; Hofmann et al., 2008; McMahon et al., 2013; Götze et al., 2020), sedimentary rocks that formed in the presence of liquid water in a potentially habitable environment represent a prime target for biosignatures. Therefore, a recurrent question during the mission will be that of differentiating outcrops of sedimentary rocks from outcrops of igneous rocks. On Mars, most outcrops are at least partially covered by regolith (i.e., a layer of loose rock particles and fragments) (Ehlmann and Edwards, 2014; Toulmin et al., 1977). For this reason, close-up images of rock textures, rather than panoramic views, may reveal essential to differentiate sedimentary rocks from igneous rocks. The habit and size of the grains constituting the rock are surely of key importance for making this differentiation, as well as to classify sedimentary and igneous rocks in their respective subcategories (Wentworth, 1922).

Besides grain/crystal shape and size, laminations are another visual feature that provides key information for classifying rocks, reconstructing depositional paleoenvironments, and identifying rocks facies that were likely deposited in the presence of liquid water. A subcategory of laminated sedimentary structures that is considered of very high interest for the scientific objectives of the ExoMars are stromatolitic laminations (e.g., Bosak et al., 2013). Stromatolites are primary sedimentary structures formed by the interaction of microbes with sediment and physical agents of erosion, deposition, and transportation (Grotzinger and Knoll, 1999). Stromatolites can be produced by very primitive microorganisms and, on Earth, they occur in sedimentary sequences that have a similar age as the Noachian rocks present at the landing site of the ExoMars rover (Allwood et al., 2006; Bontognali et al., 2012; Nutman et al., 2016). For this reason, they represent an ideal type of morphological biosignatures that may have formed early in the history of Mars and still be preserved and detectable with an instrument like CLUPI. Nevertheless, despite more than 20 years of Mars surface exploration, no laminated rock has been unambiguously interpreted as a fossil microbial mat. The presence of stromatolites at Oxia Planum remains, therefore, highly speculative.

The samples used for the simulations presented in this study were selected to have representative textures of the categories described above, including:

Apex Chert from Marble Bar, Western Australia, sedimentary rock characterized by a very homogeneous texture (no laminated or grainy texture). Silicified microfossils of early Archean age have been described from samples coming from the same outcrop, making it a good example of a sample that has no textural features but would be of interest during the ExoMars mission (Schopf, 1993). Andesite from the Eifel region, Germany, igneous rocks characterized by a texture comprised of a homogeneous matrix plus phenocrystals of different shape and size (Schmincke, 2007). The samples allow for evaluating how crystal shape and crystal detection vary depending on the working distance.

Eolian sandstone from the Lower Triassic Buntsandstein unit, Eifel region, Germany, sedimentary rocks characterized by a texture comprised of abiotically laminated clastic material (Mader, 1981).

Three different samples of stromatolites from the Tumbiana formation, Western Australia, sedimentary rocks with accretionary laminations interpreted as fossil equivalent of microbial mats (Coffey et al., 2013). These sample represent a typical Archean macroscopic morphological biosignature.

An artificially produced fine sandstone, obtained by sieving a sandstone and retaining only particles with a size ranging from 150 to 200 μm. The sand was glued on a petri-dish that could be tilted and photographed vertically simulating a sandstone exposed in an outcrop.

3. Results

The results of the simulated CLUPI images – all acquired in the configuration referred to as "close-up observation of outcrops" – are summarized in Figs. 4–7. Fig. 4 shows images of three sedimentary rocks (i.e., a black chert, an aeolian sandstone, and a stromatolite) and an igneous rock (i.e., an andesite) characterized by different textures. The images were acquired from distances ranging from 7.5 to 1 m, allowing for a qualitative evaluation of the ideal working distance necessary for recognizing a feature of interest. Similarly, Figs. 5 and 6 shows images acquired from a progressively larger distance (i.e., from 1 to 7.5 m) of an artificial sandstone (Fig. 5) and of a laminated stromatolite sample (Fig. 6). Fig. 7 includes images of another stromatolite samples and illustrates how the direction of incident light (i.e., angle between surface of interest and illumination axis) may affect recognition of rock textures and compositional heterogeneities.

4. Discussion

The first objective of our simulations was that of evaluating how clasts/crystals of different sizes and sedimentary structures can be recognized with CLUPI with a working distance ranging from 1 to 7.5 m. The rocks shown in Fig. 4 include examples of 1) a black chert without primary sedimentary structures and clasts or crystals visible in the CLUPI simulated images 2) an andesite with a porphyritic texture comprised of crystals of variable color and size but with no layering, 3) an aeolian sandstone comprised of clastic particles showing an even parallel bedding and 4) a stromatolite characterized by circular sedimentary structures (weathered domical stromatolites seen perpendicularly to the depositional plane). The figure provides a visual reference to be used by the CLUPI science team during the ExoMars prime mission, helping to quickly predict which type of image and which type of morphological detail one can expect by acquiring an image from a given distance. By looking at the set of images, it is interesting to note how some fundamental textural differences of the 4 rocks (i.e., homogeneous habit, porphyritic or clastic texture, flat laminations, stromatolitic laminations) can be perceived even from a distance at which the size of the single pixel is similar or even bigger than the size of the morphological features defining the rock facies. Although the resolution is not enough to

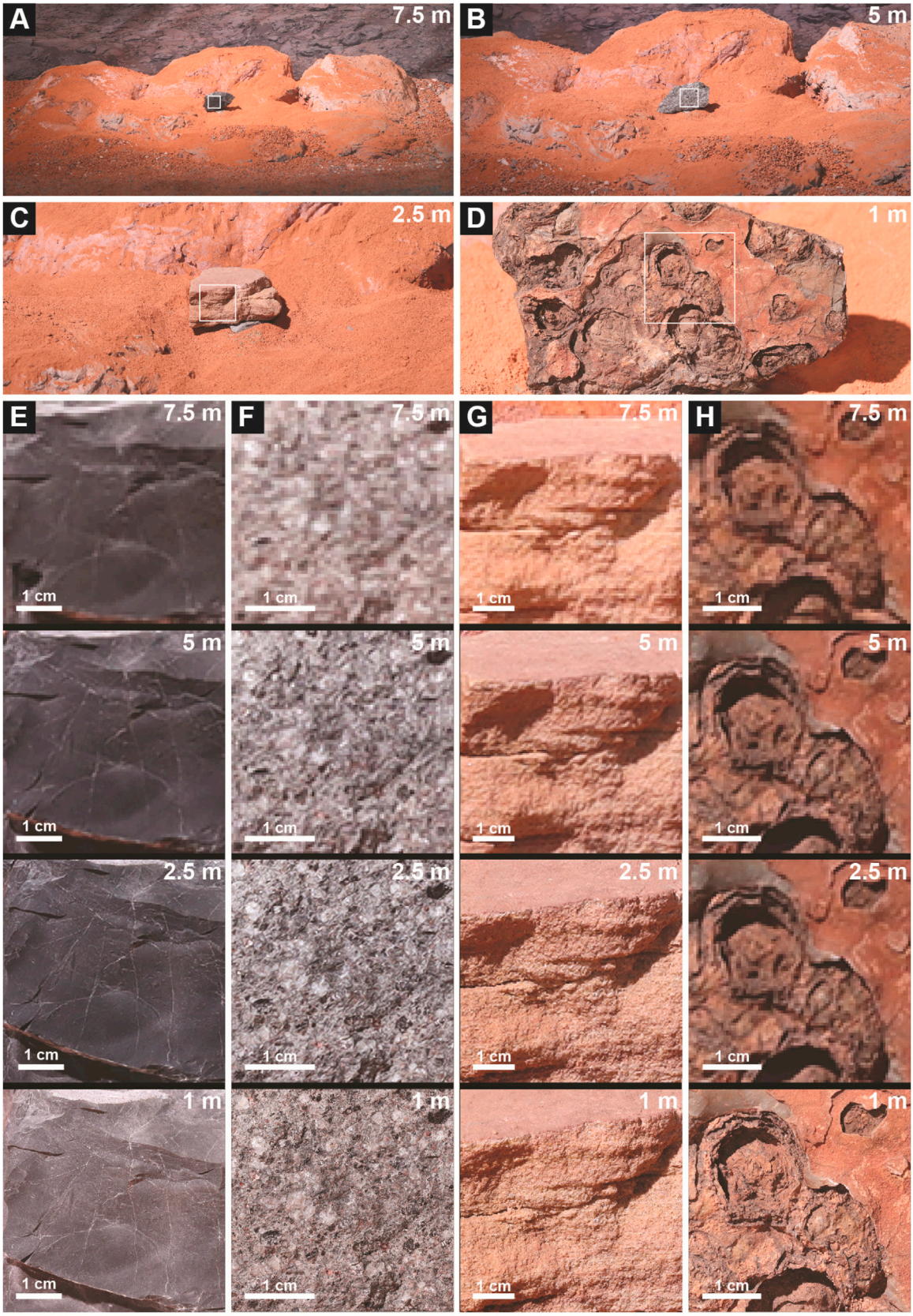

(caption on next page)

Fig. 4. Images of rock textures acquired from various distances. The figure represents a simulation of CLUPI images acquired in the configuration referred to as "close-up observation of outcrops". During this mission's science operation mode, CLUPI will look to the side using field of view 2 (FOV2), which has a resolution of 1128 × 2652 pixels. Panels A, B, C, and D show the entire FOV2. Panels E, F, G and H show only a close-up (i.e., a part of FOV2 corresponding to the white outlines, which were cropped maintaining the original number of pixels) of the same area of the sample photographed from different distances, allowing for a comparison of what textural features can be resolved by driving the rover progressively closer to the outcrop. The white number in the upper right corner indicates the distance from which the image was taken. All samples were positioned so that the orientation of the target surface had a dip of 90° (i.e., vertical) and a strike of 180° (i.e., parallel to the Marslabor back wall). All images were acquired with a measured illumination on the sample of 1000 lux of diffused light and 5000 lux of direct plus diffused light. The illumination axis (i.e., direction of incident light) had a polar angle of 45° and an azimuthal angle of 225° (i.e., the target surface was illuminated from the upper-left side). The optical axis (i.e., orientation of the camera with respect to the center of the target surface) had a polar angle of 64° in images acquired from a distance of 1 m, 79° from 2.5 m, 84° from 5 m, and 87° from 7.5 m (i.e., the camera was oriented in a slightly downward looking position). The azimuthal angle of the optical axis was 180° in all images (i.e., camera was perpendicular to the target surface). **(A & B)** Black chert with no visible clasts or laminations. **(B & F)** Andesite comprised of a matrix plus phenocrystals of different size, shape, and color. **(C & G)** Aeolian sandstone characterized by parallel laminations. **(D & H)** Stromatolites characterized by domical accretionary laminations (seen perpendicularly to the depositional plane, not in cross section).

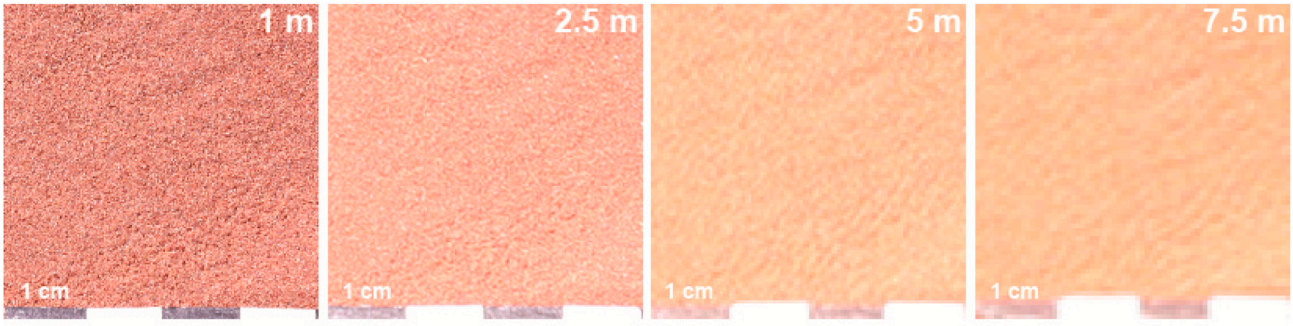

Fig. 5. Images of an artificial sandstone comprised of grains with a size ranging from 150 to 200 μm. The 4 panels of the figure are cropped portions of simulated FOV2 CLUPI images (see caption of Fig. 3 for more details) showing the same area of an artificial sandstone images from various distances (white numbers on the upper right corner of each panel). All images were acquired with a measured illumination on the sample of 1000 lux of diffused light and 5000 lux of direct plus diffused light. The sandstone grains were glued on a Petri dish that was fixed vertically on a stand. The target surface had a dip of 90° and a strike of 180°. The illumination axis had a polar angle of 34° and an azimuthal angle of 225° (i.e., the target surface was illuminated from the upper-left side). The optical axis was orthogonal to the target surface (polar angle was 90° and azimuthal angle 180°).

determine, for example, particle size or lamination thickness, the visual information appears sufficient for a preliminary interpretation of the rock. The difference between expectations base on CLUPI technical specifications (image size and resolution) and the outcome of our test based on images of actual geological samples can be explored more in detail with Figs. 5 and 6.

In Fig. 5, we present the results of a series of images of an artificially produced fine grained sandstone, which is exclusively comprised of clast with a size ranging from 150 to 250 μm (obtained by sieving a natural sandstone). Approximately 10 pixels is considered the minimum number of pixels required for determining particle size, and 50–200 pixels are necessary to describe particle shape (e.g., Cai, 2003; Kröner and Carbó, 2013). Considering that the resolution (i.e., μm/pixel) of CLUPI is 79 μm at 1 m, and 197 μm at 2.5 m, one would predict that a fine grained sandstone like that photographed requires a working distance of not more than about 2 m to be recognized. Our test shows that despite this statement is true if the goal of the image is a characterization of particle size, images taken at distance higher than 2.5 m are still valuable for differentiating a putative fine-grain sandstone from an aphanitic basalt, two rocks that have a significantly different potential of preserving biosignatures. Indeed, although the pixel's size surpasses the size of the grain constituting the rock, a grainy texture is evident even from the picture taken from 7.5 m (Fig. 5). The resolution is not sufficient to make a scientifically robust classification of the rock. In fact, from 7.5 m the texture appears coarser than the actual one. However, the image may still be of help to the operational team for planning the subsequent movements of the rover, deciding whether to move closer to a potentially interesting target or continuing a traverse without losing time.

A similar conclusion can be drawn with the series of images of a stromatolite sample presented in Fig. 6. From a distance of 7.5 m, a pixel corresponds to 592 μm, which is not sufficient to resolve the thickness of the layers defining the lamination (Fig. 5J-K-L). Indeed, if compared to the images taken from a closer distance, that taken from 7.5 m does not allow for identifying a continuous layer and evaluating the morphology and angular relationships among the alternating laminae, which is essential to assess the possible biogenicity of the sedimentary structure. Nevertheless, the general "putative stromatolitic texture" is sufficiently different from that characterizing a non-laminated or flat-laminated rock formation photographed from the same distance (compare with Fig. 4).

Among the factors that play a role and needs to be considered for improving predications on what rock facies can be differentiated from a given distance, illumination surely play an important role. This is illustrated with Fig. 7, in which the same stromatolite sample has been photographed from the same position but with the spot light for simulating direct light placed in different positions (i.e., simulating different angle between the illumination axis and the target surface). In this example, a lateral illumination (i.e., illumination axis almost parallel to the target surface) allows for a better recognition of textural features due to the topography of the surface of the sample (e.g., lamination emphasized by differential resistance to erosion or secondary alteration features) (Fig. 7A-B-C). Instead, a perpendicular illumination (i.e., illumination axis perpendicular to the target surface) appears better for recognizing mineralogical/compositional heterogeneities that are emphasized more by differences in color rather than topography (Fig. 7C-D-E). This information may help the CLUPI/ExoMars science team to select the ideal time of the day for telecommanding the acquisition of an image (e.g., midday light vs morning or afternoon light) or to decide how to drive and orient the rover with respect to the sun during the approach of a geological outcrop.

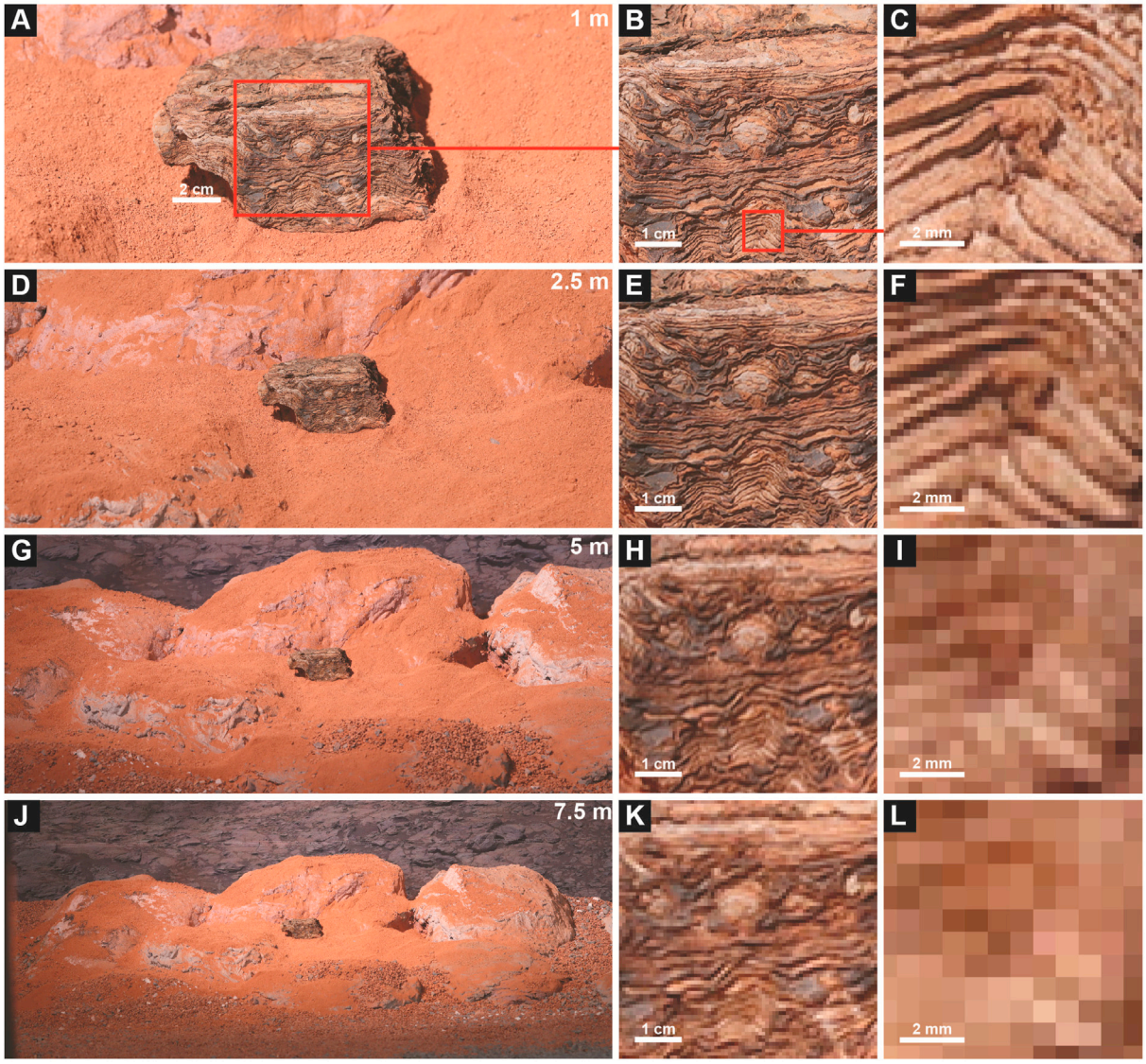

Fig. 6. Images of a Tumbiana stromatolite sample. Simulated CLUPI images acquired from different distances using the operation's configuration "close-up observation of outcrops", allowing for a comparison of how the stromatolitic laminations are visible from progressively larger distance. (**A, D, G, and J**) Entire CLUPI field of view 2 (FOV2, i.e., 1128 × 2652 pixels). The white number on the upper right corner indicates the distance from which the picture was acquired. **(B, C, E, F H, I, K, L)** Close-ups (i.e., a cropped and enlarged portion without modifying the number of pixels) of the images on the left. All images were acquired with a measured illumination on the sample of 1000 lux of diffused light and 5000 lux of direct plus diffused light. The illumination axis (i.e., direction of incident light) had a polar angle of 45° and an azimuthal angle of 225° (i.e., the target surface was illuminated from the upper-left side). The optical axis (i.e., orientation of the camera with respect to the center of the target surface) had a polar angle of 64° in images acquired from a distance of 1 m, 79° from 2.5 m, 84° from 5 m, and 87° from 7.5 m (i.e., the camera was oriented in a slightly downward-looking position). The azimuthal angle of the optical axis was 180° in all images (i.e., the camera was perpendicular to the target surface).

5. Conclusions

This first series of simulations allowed us to produce images of geological samples that will help the CLUPI/ExoMars science team in the daily tactical planning of the rover during the mission on Mars. It is important to note that the images presented in this article were obtained with a commercial camera that reproduces the CLUPI spatial resolution and viewed area, but which does not have the same detector, optics, and color calibration process. Although not identical –mostly in terms of color and depth of field– to those of the CLUPI flight model, the images produced with the commercial camera allow for approximately predicting what kind of visual information can be expected by acquiring images of geological samples from a given distance. Moreover, these preliminary results emphasize the importance of conducting simulations with actual geological samples. Indeed, in most of the simulations, sedimentary structures and rock textures tend to be recognizable even from distances that are larger than those one would predict based on the resolution of the instrument and the size of the structure or particles that defines the rock texture or sedimentary structures (e.g., a clastic sedimentary rock can be recognized even when it is comprised of particles that are smaller than the size of the pixels constituting the image). Identifying minimal image-acquisition-distances necessary for identifying relevant rock facies is important for optimizing the scientific return of a mission like ExoMars. In a mission in which rover movements and data transmission are limited, finding the best balance between "exploring a wider possible area" and "not driving-by interesting outcrops without noticing them" remains a fundamental objective. By expanding the dataset in order to produce a more comprehensive catalogue of Mars analogue rocks, it will also be possible to understand common sources of bias and error and consider them during the elaboration next generation rock-recognition

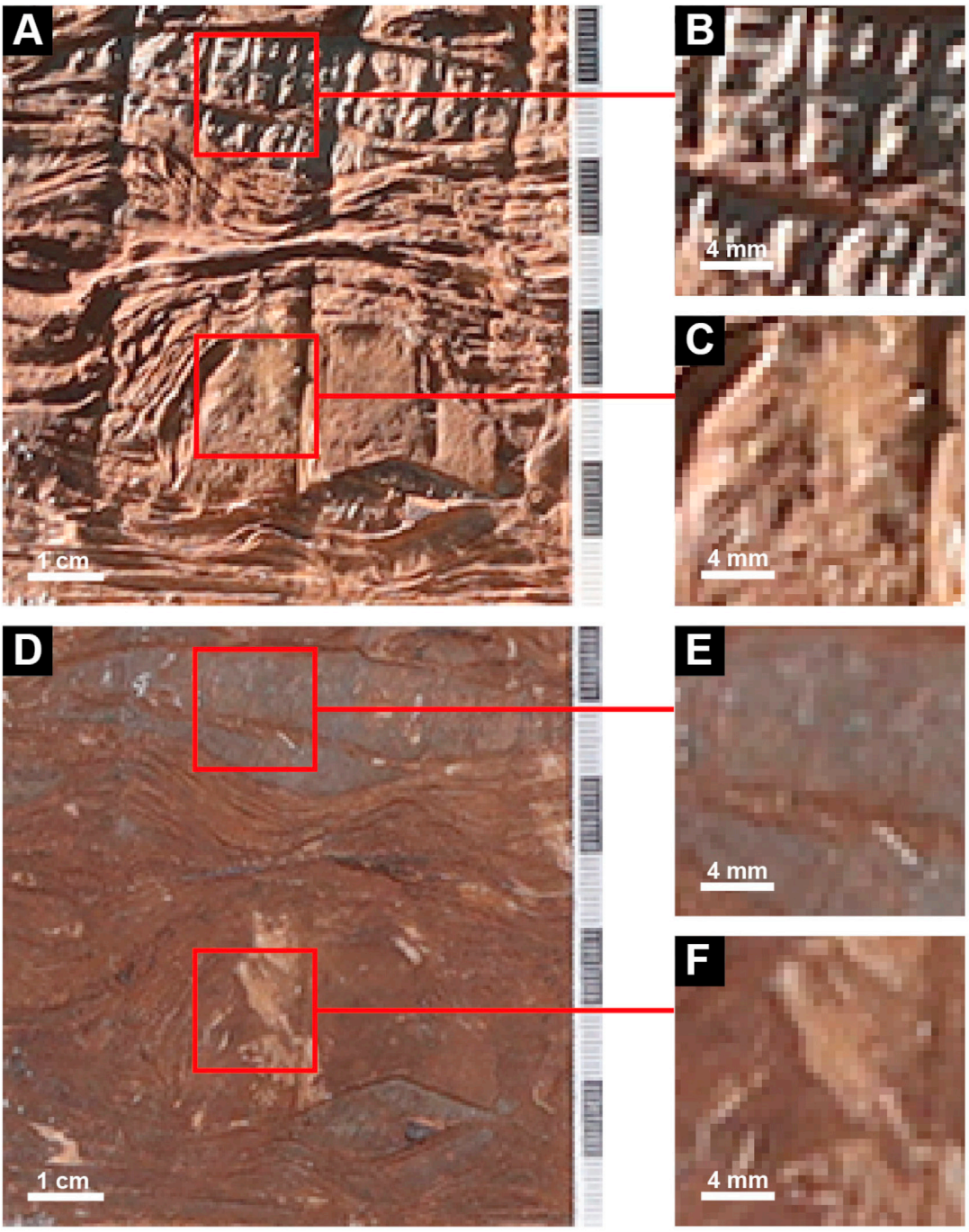

Fig. 7. Tumbiana stromatolite sample photographed under different incident light conditions. The figure's panels are cropped portions of simulated FOV2 CLUPI images (see caption of Fig. 3 for more details) of a stromatolite sample, which allows for evaluating how the direction of incident light (i.e., angle between surface of interest and illumination axis) affects recognition of rock textures and compositional heterogeneities. All photos were acquired from a distance of 5 m. **(A)** Image acquired with a measured illumination on the sample of 1000 lux of diffused light and 5000 lux of direct plus diffused light. The illumination axis had a polar angle of 79° and an azimuthal angle of 262° (i.e., illumination from the left-side almost parallel to the target surface). **(B & C)** Close-ups obtained by cropping and enlarging the two areas (red squares) of panel (A) without modifying the original number of pixels. **(D)** Image acquired with a measured illumination on the sample of 1000 lux of diffused light and 5000 lux of direct plus diffused light. The illumination axis had a polar angle of 79° and an azimuthal angle of 180° (i.e., illumination perpendicular to the target surface). **(E & F)** Close-ups of (D).

approaches.

Author statement

Tomaso R.R. Bontognali: Conceptualization, Methodology, Investigation, Resources, Writing - Original Draft, Visualization. Yardena Meister: Methodology, Investigation, Writing - Review & Editing. Brigitte Kuhn: Methodology, Investigation. Jean-Luc Josset: Conceptualization, Resources, Writing - Review & Editing, Funding acquisition. Beda A. Hofmann: Conceptualization, Resources, Writing - Review & Editing. Nikolaus Kuhn: Conceptualization, Investigation, Resources, Writing - Review & Editing, Project administration, Funding acquisition.

Declaration of competing interest

The authors declare that they have no known competing financial interests or personal relationships that could have appeared to influence the work reported in this paper.

Acknowledgments

We thank Mitchell Schulte and Martin Van Kranendonk for having organized the field trip in the Pilbara region (Western Australia) during which we had the opportunity to collected the stromatolite samples used for the CLUPI simulations presented in this study. This work was supported by the Swiss National Science Foundation (grant 200021_197293), by the internal funding of the University of Basel, and by the internal funding of the Space Exploration Institute.

References

Allwood, A.C., Walter, M.R., Kamber, B.S., Marshall, C.P., Burch, I.W., 2006. Stromatolite reef from the early Archaean era of Australia. Nature 441, 714–718. https://doi.org/10.1038/nature04764.

Appelbaum, J., Flood, D.J., 1990. Solar radiation on Mars. Solar Energy 45 (6), 353–363, 90006-A. https://doi.org/10.1016/0038-092X(90)90156-7.

Bontognali, T.R.R., D'Angeli, I.M., Tisato, N., Vasconcelos, C., Bernasconi, S.M., Gonzales, E.R., De Waele, J., 2016. Mushroom speleothems: stromatolites that formed in the absence of phototrophs. Front. Earth Sci. 4, 49.

Bontognali, T.R.R., Sessions, A.L., Allwood, A.C., Fischer, W.W., Grotzinger, J.P., Summons, R.E., Eiler, J.M., 2012. Sulfur isotopes of organic matter preserved in 3.45-billion-year-old stromatolites reveal microbial metabolism. Proc. Natl. Acad. Sci. Unit. States Am. 109, 15146–15151. https://doi.org/10.1073/pnas.1207491109.

Bosak, T., Knoll, A.H., Petroff, A.P., 2013. The meaning of stromatolites, 41, 21 2012 Annu. Rev. Earth Planet Sci.. https://doi.org/10.1089/153110703769016442.

Cady, S.L., Farmer, J.D., Grotzinger, J.P., Schopf, J.W., Steele, A., 2003. Morphological biosignatures and the search for life on Mars. Astrobiology 3 (2), 351–368.

Cai, Y., 2003. How many pixels do we need to see things?. In: International Conference on Computational Science. Springer, Berlin, Heidelberg, pp. 1064–1073.

Coffey, J.M., Flannery, D.T., Walter, M.R., George, S.C., 2013. Sedimentology, stratigraphy and geochemistry of a stromatolite biofacies in the 2.72 Ga Tumbiana formation, Fortescue Group, Western Australia. Precambrian Res. 236, 282–296.

Davies, N.S., Liu, A.G., Gibling, M.R., Miller, R.F., 2016. Resolving MISS conceptions and misconceptions: a geological approach to sedimentary surface textures generated by microbial and abiotic processes. Earth Sci. Rev. 154, 210–246. https://doi.org/10.1016/j.earscirev.2016.01.005.

Edgett, K.S., Yingst, R.A., Ravine, M.A., Caplinger, M.A., Maki, J.N., Ghaemi, F.T., Schaffner, J.A., Bell, J.F., Edwards, L.J., Herkenhoff, K.E., Heydari, E., Kah, L.C., Lemmon, M.T., Minitti, M.E., Olson, T.S., Parker, T.J., Rowland, S.K., Schieber, J., Sullivan, R.J., Sumner, D.Y., Thomas, P.C., Jensen, E.H., Simmonds, J.J., Sengstacken, A.J., Willson, R.G., Goetz, W., 2012. In: Yingst, S., Ravine, R.A., Caplinger, M.A., Maki, M.A., Ghaemi, J.N. (Eds.), Curiosity, pp. 259–317. https://doi.org/10.1007/s11214-012-9910-4.

Ehlmann, B.L., Edwards, C.S., 2014. Mineralogy of the martian surface. Annu. Rev. Earth Planet Sci. 42 (1), 291–315. https://doi.org/10.1146/annurev-earth-060313-055024.

Götze, J., Hofmann, B., Machałowski, T., Tsurkan, M.V., Jesionowski, T., Ehrlich, H., Kleeberg, R., Ottens, B., 2020. Biosignatures in subsurface filamentous fabrics (SFF) from the Deccan volcanic Province, India. Minerals 20. https://doi.org/10.3390/min10060540.

Grotzinger, J.P., Knoll, A.H., 1999. Stromatolites in Precambrian carbonates: evolutionary mileposts or environmental dipsticks? Annu. Rev. Earth Planet Sci. 27 (1), 313–358.

Hofmann, B.A., Farmer, J.D., von Blanckenburg, F., Fallick, A.E., 2008. Subsurface filamentous fabrics: an evaluation of possible modes of origins based on morphological and geochemical criteria, with implications for exopalaeontology. Astrobiology 8, 87–117.

Homann, M., 2019. Earliest life on Earth: evidence from the Barberton Greenstone Belt, South Africa. Earth Sci. Rev. 196, 102888. https://doi.org/10.1016/j.earscirev.2019.102888.

Josset, J.-L., Westall, F., Hofmann, B.A., Spray, J., Cockell, C., Kempe, S., Griffiths, A.D., De Sanctis, M.C., Colangeli, L., Koschny, D., Föllmi, K., Verrecchia, E., Diamond, L., Josset, M., Javaux, E.J., Esposito, F., Gunn, M., Souchon-Leitner, A.L., Bontognali, T.R.R., Korablev, O., Erkman, S., Paar, G., Ulamec, S., Foucher, F., Martin, P., Verhaeghe, A., Tanevski, M., Vago, J.L., 2017. The close-up imager onboard the ESA ExoMars rover: objectives, description, operations, and science validation activities. Astrobiology 17, 595–611. https://doi.org/10.1089/ast.2016.1546.

Kröner, S., Carbó, M.T.D., 2013. Determination of minimum pixel resolution for shape analysis: proposal of a new data validation method for computerized images. Powder Technol. 245, 297–313.

Mader, D., 1981. Genesis of the buntsandstein (lower triassic) in the Western Eifel (Germany). Sediment. Geol. 29 (1), 1–30.

Mandon, L., Parkes Bowen, A., Quantin-Nataf, C., Bridges, J.C., Carter, J., Pan, L., et al., 2021. Morphological and spectral diversity of the clay-Bearing unit at the ExoMars landing site Oxia planum. Astrobiology 21 (4), 464–480.

McMahon, S., Parnell, J., Ponicka, J., Hole, M., Boyce, A., 2013. The habitability of vesicles in martian basalt. Astron. Geophys. 54, 1.17-1.21.

Noffke, N., 2009. The criteria for the biogeneicity of microbially induced sedimentary structures (MISS) in Archean and younger, sandy deposits. Earth-Sci. Rev., Microbial Mats in Earth's Fossil Record of Life: Geobiology 96, 173–180. https://doi.org/10.1016/j.earscirev.2008.08.002.

Nutman, A.P., Bennett, V.C., Friend, C.R.L., Van Kranendonk, M.J., Chivas, A.R., 2016. Rapid emergence of life shown by discovery of 3,700-million-year-old microbial structures. Nature 537 (7621), 535–538. https://doi.org/10.1038/nature19355.

Quantin-Nataf, C., Carter, J., Mandon, L., Thollot, P., Balme, M., Volat, M., et al., 2021. Oxia planum: the landing site for the ExoMars "Rosalind Franklin" rover mission: geological context and prelanding interpretation. Astrobiology 21 (3), 345–366.

Ross, K.A., Fisher, R.V., 1986. Biogenic grooving on glass shards. Geology 14 (7), 571–573.

Schmincke, H.U., 2007. The Quaternary volcanic fields of the east and west Eifel (Germany). In: Mantle plumes. Springer, Berlin, Heidelberg, pp. 241–322.

Vago, J., Witasse, O., Svedhem, H., Baglioni, P., Haldemann, A., Gianfiglio, G., Blancquaert, T., McCoy, D., de Groot, R., 2015. ESA ExoMars program: the next step in exploring Mars. Sol. Syst. Res. 49, 518phys. Res. 1896-1977 82,.1134/S0038094615070199.

Schopf, J.W., 1993. Microfossils of the early Archean Apex chert: new evidence of the Antiquity of life. Science 260 (5108), 640–646. https://doi.org/10.1126/science.260.5108.640.

Toulmin, III., Baird, A.K., Clark, B.C., Keil, K., Rose, Christian, R.P., Evans, P.H., Kelliher, W.C., 1977. Geochemical and mineralogical interpretation of the Viking inorganic chemical results. J. Geophys. Res. 82 (28), 4625–4634.

Pasteur Instrument Teams, L.S.S.W.G., and Other Contributors Vago, J.L., Westall, F., Coates, A.J., Jaumann, R., Korablev, O., Ciarletti, V., Mitrofanov, I., Josset, J.-L., De Sanctis, M.C., Bibring, J.-P., Rull, F., Goesmann, F., Steininger, H., Goetz, W., Brinckerhoff, W., Szopa, C., Raulin, F., Westall, F., Edwards, H.G.M., Whyte, L.G., Fairén, A.G., Bibring, J.-P., Bridges, J., Hauber, E., Ori, G.G., Werner, S., Loizeau, D., Kuzmin, R.O., Williams, R.M.E., Flahaut, J., Forget, F., Vago, J.L., Rodionov, D., Korablev, O., Svedhem, H., Sefton-Nash, E., Kminek, G., Lorenzoni, L., Joudrier, L., Mikhailov, V., Zashchirinskiy, A., Alexashkin, S., Calantropio, F., Merlo, A., Poulakis, P., Witasse, O., Bayle, O., Bayón, S., Meierhenrich, U., Carter, J., García-Ruiz, J.M., Baglioni, P., Haldemann, A., Ball, A.J., Debus, A., Lindner, R., Haessig, F., Monteiro, D., Trautner, R., Voland, C., Rebeyre, P., Goulty, D., Didot, F., Durrant, S., Zekri, E., Koschny, D., Toni, A., Visentin, G., Zwick, M., van Winnendael, M., Azkarate, M., Carreau, C., the ExoMars Project Team, 2017. Habitability on early Mars and the search for biosignatures with the ExoMars rover. Astrobiology 17, 471–510. https://doi.org/10.1089/ast.2016.1533.

Wentworth, C.K., 1922. A scale of grade and class terms for clastic sediments. J. Geol. 30, 377–392.

Westall, F., Foucher, F., Bost, N., Bertrand, M., Loizeau, D., Vago, J.L., Kminek, G., Gaboyer, F., Campbell, K.A., Bréhéret, J., Gautret, P., Cockell, C.S., 2015. Biosignatures on Mars: what, where, and how? Implications for the search for martian life. Astrobiology 15 (11), 998–1029.